Lokeshwar, V. B., Huang, S. S., & Huang, J. S. (1989) *J. Biol. Chem. 264*, 19318-19326.
Marsh, L., & Herskowitz, I. (1988) in *Cold Spring Harbor Symposia on Quantitative Biology*, Vol. LIII, pp 557-565, Cold Spring Harbor, NY.
Masui, Y., Chino, N., Sakakibara, S., Tanaka, T., Murakami, T., & Kita, H. (1977) *Biochem. Biophys. Res. Commun. 78*, 534-538.
Mayo, K. H., Nunez, M., Burke, C., Starbuck, C., Lauffenburger, D., & Savage, C. C. (1989) *J. Biol. Chem. 264*, 17838-17844.
Miyajima, I., Nakafuku, M., Nakayama, N., Brenner, C., & Miyajima, A. (1987) *Cell 50*, 1011-1019.
Naider, F. R., Jelicks, L. A., Becker, J. M., & Broido, M. S. (1989) *Biopolymers 28*, 487-497.
Nakayama, N., Miyajima, A., & Arai, K. (1985) *EMBO J. 4*, 2643-2648.
Olah, M., & Stiles, G. L. (1990) *J. Neurochem. 55*, 1432-1438.
Raths, S. K., Naider, F. R., & Becker, J. M. (1988) *J. Biol. Chem. 263*, 17333-17341.
Reneke, J. E., Blumer, K. J., Courchesne, W. E., & Thorner, J. (1988) *Cell 55*, 221-234.
Schlessinger, J. (1988) *Biochemistry 27*, 3119-3123.
Shenbagamurthi, P., Baffi, R., Khan, S. A., Becker, J. M., & Naider, F. (1983) *Biochemistry 22*, 1298-1304.
Shenbagamurthi, P., Kundu, B., Raths, S., Becker, J. M., & Naider, F. (1985) *Biochemistry 24*, 7070-7076.
Sprague, G. F., & Herskowitz, I. (1981) *J. Mol. Biol. 153*, 305-321.
Stotzler, D., Betz, R., & Duntze, W. (1977) *J. Bacteriol. 132*, 28-35.
Unson, C. G., MacDonald, D., Ray, K., Durrah, T. L., & Merrifield, R. B. (1991) *J. Biol. Chem. 266*, 2763-2766.
Weiland, G. A., Minneman, K. P., & Molinoff, P. B. (1988) *Nature 281*, 114-117.
Whiteway, M., Hougan, L., Dignard, D., Bell, L., Saari, G., Grant, F., O'Hara, P., & MacKay, V. L. (1989) *Cell 56*, 467-477.
Xue, C.-B., Bargiota, E. E., Miller, D., Becker, J. M., & Naider, F. (1989) *J. Biol. Chem. 264*, 19161-19168.

Interactions of Acyl-Coenzyme A with Phosphatidylcholine Bilayers and Serum Albumin†

John G. Boylan* and James A. Hamilton
Biophysics Department, Housman Medical Research Center, Boston University School of Medicine, 80 East Concord Street, Boston, Massachusetts 02118-2394

Received June 28, 1991; Revised Manuscript Received October 2, 1991

ABSTRACT: Interactions of oleoyl- and octanoyl-coenzyme A (CoA) with phosphatidylcholine (PC) vesicles and bovine serum albumin (BSA) were investigated by NMR spectroscopy. Binding of acyl-CoA to small unilamellar PC vesicles and to BSA was detected by changes in ^{13}C and ^{31}P chemical shifts relative to the chemical shifts for aqueous acyl-CoA. When oleoyl-CoA (≤15 mol %) was added to preformed vesicles, the ^{13}C thioester signal (200.1 ppm) was upfield from the signal for micellar oleoyl-CoA (201.7 ppm), suggesting decreased H-bonding (partial dehydration) at the carbonyl group upon binding to the bilayer. When vesicles were prepared by cosonication of oleoyl-CoA and PC, a second peak (199.8 ppm) was seen. The major peak at 200.1 ppm broadened and shifted after addition of $Dy(NO_3)_3$ and was not seen after addition of BSA, while the peak at 199.8 ppm was unaffected by either perturbation. Thus, oleoyl-CoA in each bilayer leaflet was distinguished, and transbilayer movement was shown to be slow ($t_{1/2} \geq$ hours). PC vesicles remained intact with ≤15 mol % oleoyl-CoA, while higher oleoyl-CoA proportions produced mixed micelles. In contrast, ^{13}C spectra revealed rapid exchange (ms) of octanoyl-CoA between the aqueous phase and PC vesicles and a low affinity for the bilayer. Thus, the binding affinity of acyl-CoA for PC bilayers is dependent on the acyl chain length. Oleoyl-CoA in the presence of BSA (1 mol/mol) gave rise to three carbonyl signals at 197.2-203.6 ppm. With 2-5 mol of oleoyl-CoA/BSA, 1-2 additional signals were observed. None of the signals corresponded to unbound oleoyl-CoA. Addition of [^{13}C]carboxyl-enriched oleic acid to oleoyl-CoA/BSA mixtures revealed simultaneous binding of oleic acid and oleoyl-CoA to BSA, with some perturbation of binding interactions. Thus, BSA contains multiple binding sites for oleoyl-CoA and can bind fatty acid and acyl-CoA simultaneously.

Fatty acid thioesters of coenzyme A (acyl-CoA)[1] are important intermediates in fatty acid metabolism and lipid biosynthesis. They are powerful inhibitors of several enzymes (Bortz & Lynen, 1963a; Caggiano & Powell, 1979) and may play an important regulatory role in a variety of biochemical processes, such as adenine nucleotide transport across mitochondrial membranes (Shug & Shrago, 1973). Their regulatory effects appear to be independent of their detergent-like properties, since many enzymes are inhibited by acyl-CoA below the critical micelle concentration (CMC). Furthermore,

† Supported by Grants HL26335 and HL07224 from National Institutes of Health.
* To whom correspondence should be addressed.

[1] Abbreviations: BSA, bovine serum albumin; CMC, critical micelle concentration; CoA, coenzyme A; EM, electron microscopy; NMR, nuclear magnetic resonance (spectroscopy); NOE, nuclear Overhauser enhancement; PC, phosphatidylcholine; THF, tetrahydrofuran; TLC, thin layer chromatography.

0006-2960/92/0431-557$03.00/0

long-chain acyl-CoA has a high affinity for phospholipid bilayers (Powell et al., 1985) and some proteins (Sumper & Trauble, 1973; Burrier et al., 1987) and thus may not normally be present in concentrations sufficient to form micelles. High levels of acyl-CoA do accumulate in certain pathological states, however, and may cause irreversible damage to cellular membranes. Examples include heart muscle following ischemia (Whitmer et al., 1978) and liver during starvation (Bortz & Lynen, 1963b).

Little is known about the interactions of acyl-CoA with these tissues or its effects on the progress of membrane damage. For this reason, ^{13}C and ^{31}P NMR spectroscopy were used to investigate the interactions of acyl-CoA with model membranes and to determine the proportion of acyl-CoA which disrupts phospholipid bilayer structures. The oleoyl ester of coenzyme A was studied as a representative long-chain acyl-CoA and the octanoyl ester as a medium-chain representative. ^{13}C NMR was used as a sensitive probe of the local environment of the fatty acyl carbonyl group; the ^{13}C chemical shift provides information about its hydrogen-bonding and local polarity (Hutton et al., 1977; Hamilton & Small, 1981). ^{31}P NMR was used to probe the interactions and mobility of the polar CoA moiety in different environments. The interactions of acyl-CoA with bovine serum albumin (BSA), a protein which is known to exhibit high-affinity binding of acyl-CoA in vitro (Richards et al., 1990), were also investigated. ^{13}C NMR is a potent method for detecting distinct microenvironments of lipids in the heterogeneous binding sites of albumin (Parks et al., 1983). The results of this study provide new details of interactions of acyl-CoA with membranes and proteins. A preliminary account of this work has been published (Boylan & Hamilton, 1990).

Materials and Methods

Materials. Egg yolk phosphatidylcholine (PC) was purchased from Avanti Polar Lipids (Pelham, AL) and used without further purification. 99% [1-^{13}C]oleic acid and 99% [1-^{13}C]octanoic acid were purchased from Cambridge Isotope Laboratories (Cambridge, MA). Essentially fatty acid-free bovine serum albumin (BSA), coenzyme A (CoA), unenriched octanoyl- and oleoyl-CoA, and Dowex-50W (H+) were purchased from Sigma Chemical Co. (St. Louis, MO). 1,1'-Carbonyldiimidazole, copper(I) chloride, aluminum oxide (activated, basic, Brockmann I), tetrahydrofuran (THF), and calcium hydride were purchased from Aldrich Chemical Co. (Milwaukee, WI).

[1-^{13}C]Oleic acid was purified by dissolving it in benzene/chloroform/methanol (1.0:0.5:1.2 v/v/v) and adding NaOH. The resulting sodium salt was extracted in the aqueous phase, HCl was added, and the fatty acid was finally extracted in hexane (Burrier & Brecher, 1983). The oleic acid was judged to be >99% pure by TLC on silica gel. THF was treated for peroxides by refluxing in copper(I) chloride and distilling from calcium hydride. Diethyl ether was dried and treated for peroxides by passing it through aluminum oxide just prior to use. All other reagents were used without further purification.

Synthesis. [1-^{13}C]Oleoyl-CoA and [1-^{13}C]octanoyl-CoA were synthesized using the method of Kawaguchi et al. (1981), in which the fatty acid is reacted with carbonyldiimidazole in anhydrous THF and the resulting 1-acylimidazolide is then reacted with CoA in THF/H_2O (2:1 v/v) to give the thioester. A ratio of 1 mol of [1-^{13}C]fatty acid to 2 mol each of 1,1'-carbonyldiimidazole and CoA was used. The crude oleoyl-CoA (containing some unreacted CoA, imidazole, and free fatty acid) was purified by washing three times each with cold $HClO_4$ (1.3% v/v), dry acetone, and dry diethyl ether (Bishop & Hajra, 1980). The crude octanoyl-CoA could not be purified in the same way since its solubility in $HClO_4$ was found to be unacceptably high. Instead, octanoyl-CoA was washed 3× in diethyl ether and purified by preparative TLC on plates containing 0.1-mm microgranular cellulose with a mobile phase of 1-butanol/water/acetic acid (50:30:20 v/v/v). The purity of both thioesters was judged to be >99% by TLC against unlabeled acyl-CoA standards. ^{13}C NMR spectra of micellar (oleoyl) and monomeric (octanoyl) ^{13}C-enriched acyl-CoA showed a single thioester carbonyl peak for each.

Sample Preparation. Aqueous samples were prepared by dissolving the lyophilized acyl-CoA in 50 mM aqueous potassium phosphate buffer at pH 7.2–7.4. PC vesicles were prepared as previously described (Hamilton & Small, 1981) in 50 mM potassium phosphate at pH 7.4. Selected samples were examined before and after NMR analysis by negative-stain electron microscopy (EM) on glow-discharged carbon-coated copper Formvar grids as previously described (Hamilton, 1989) except that the vesicles were diluted 50- or 100-fold in 50 mM potassium phosphate at pH 7.4. Acyl-CoA/PC mixtures were prepared by (i) adding aqueous acyl-CoA to small unilamellar PC vesicles ("preformed vesicles") or (ii) mixing lyophilized acyl-CoA with dry PC, adding buffer, vortexing to hydrate the lipid, and then sonicating the cloudy lipid mixture to transparency ("cosonicated vesicles"). BSA was dissolved in 50 mM potassium phosphate at pH 7.4 and filtered through a 0.2-μm filter (Acrodisc; Gelman Sciences, Ann Arbor). The concentration was determined from the absorbance at 279 nm (Janatova et al., 1968). Acyl-CoA/BSA mixtures at different mole ratios were prepared by adding known amounts of aqueous acyl-CoA to a fixed amount of BSA or by preparing a sample containing a high mole ratio of acyl-CoA to albumin and diluting with BSA. NMR results were identical in either case. Potassium oleate was prepared as previously described (Parks et al., 1983) and added to oleoyl-CoA/BSA mixtures or to BSA before addition of oleoyl-CoA to make oleoyl-CoA/oleic acid/BSA mixtures. Large unilamellar vesicles were prepared from PC by hydrating the dried lipid in 50 mM potassium phosphate buffer, vortexing followed by three freeze/thaw cycles, and then passing the dispersion through 0.4-μm (2×) and 0.1-μm (3×) polycarbonate filters (Nucleopore, Pleasanton, CA).

In selected samples, the concentrations of oleoyl-CoA, PC, and BSA were determined by chemical analysis before and after NMR analysis. Oleoyl-CoA was estimated using acyl-CoA oxidase (Mizuno et al., 1980); PC was determined using a modified phospholipase D method (Tokayama et al., 1977); and BSA was determined using the Lowry method (Lowry et al., 1951). All samples were adjusted to pH 7.4 ± 0.1 (with 0.1 N NaOH or 0.1 N HCl as needed) before NMR analysis.

NMR Methods. ^{13}C and ^{31}P NMR spectra were obtained at 50.3 and 81.0 MHz, respectively, on a Bruker WP-200 spectrometer equipped with an Aspect 2000A computer as previously described (Hamilton & Small, 1981). ^2H_2O was used as an internal lock signal. In samples which contained PC, ^{13}C chemical shifts were measured using the fatty acyl methyl resonance at 14.10 ppm (relative to tetramethylsilane) as an internal reference. In all other samples, an insert containing tetramethylsilane in $CHCl_3$ was used as an external chemical shift reference; 0.20 ppm was added to chemical shifts measured in these samples for comparison with chemical shifts based on internal referencing of the fatty acyl methyl (Hamilton & Cistola, 1986). ^{31}P chemical shifts were measured

relative to the signal from 85% H_3PO_4 (0.0 ppm) contained in a capillary insert. Generally, the insert was removed from the sample for the final spectrum because of overlap of the inorganic ^{31}P signal with sample peak(s). Spin–lattice relaxation times (T_1) were measured by using a fast inversion–recovery pulse program (Canet et al., 1975); ^1H–^{13}C nuclear Overhauser enhancements (NOE) were measured by comparing peak intensities of spectra recorded with broad-band and inverse-gated ^1H decoupling (Opella et al., 1976). The composition of selected acyl-CoA/PC samples was determined directly from the NMR spectrum from the ratio of peak areas of the acyl-CoA/PC carbonyl signals. Peak intensities were measured under equilibrium pulsing conditions (pulse interval $> 4 \times T_1$) and corrected for the different number of carbon atoms contributing to the peak (two for PC, one for acyl-CoA), the ^{13}C abundance (1.1% for PC, 99% for acyl-CoA), and the experimentally determined NOE (1.68 for PC, 1.74 for oleoyl-CoA and octanoyl-CoA). For a 5 mol % oleoyl-CoA/PC sample, for example, this ratio should be

[5 mol % oleoyl-CoA × 1 carbonyl × 0.99 (^{13}C abundance) × 1.74 NOE]/[95 mol % PC × 2 carbonyls × 0.011 (^{13}C abundance) × 1.68 NOE] = 2.45

Titration Spectra of Oleoyl-CoA. ^{31}P NMR spectra were recorded for micellar oleoyl-CoA, oleoyl-CoA bound to PC, and oleoyl-CoA bound to BSA over the pH range of 3.95–9.25. Each sample contained 4.5 mM oleoyl-CoA in 50 mM KCl. The PC sample contained 5 mol % oleoyl-CoA and 95 mol % PC, and the BSA sample contained a 3:1 mole ratio of oleoyl-CoA to BSA. Chemical shifts were measured relative to 85% H_3PO_4 (external) and, along with corresponding pH values, were fit to an equation derived from the Henderson–Hasselbach equation and modified for NMR titrations:

$$\delta = \frac{\delta_{max} - [\delta_{min} \times \log^{-1}(pH - pK)]}{1 + \log^{-1}(pH - pK)}$$

where δ is the observed chemical shift, δ_{max} is the maximum chemical shift (fully ionized), and δ_{min} is the minimum chemical shift (fully protonated).

Results

Monomeric/Micellar Forms. ^{13}C NMR spectra were obtained for aqueous samples of oleoyl-CoA and octanoyl-CoA at 35 °C. Carbonyl chemical shifts were measured over a concentration range encompassing the estimated critical micelle concentration (CMC) of octanoyl-CoA (~35 mM; see Discussion). ^{13}C-enriched octanoyl-CoA was used for lower concentrations (1–20 mM) and unenriched octanoyl-CoA for higher concentrations (55–110 mM). Since the CMC of oleoyl-CoA is very low (~30 μM; Smith & Powell, 1986), it was possible to measure only the micellar chemical shift (1–20 mM), even with ^{13}C enrichment. Both oleoyl-CoA and octanoyl-CoA exhibited narrow carbonyl NMR peaks far downfield of typical fatty acyl carbonyls, at 201.7 ppm (Figure 1A) for micellar oleoyl-CoA and at 200.3 ppm for micellar octanoyl-CoA. The chemical shift determined for micellar oleoyl-CoA is close to that previously reported for palmitoyl-CoA at pH 6.6 (201.09 ppm; Maggio, 1980). The chemical shift of monomeric octanoyl-CoA (205.4 ppm, Figure 1B) was significantly downfield of micellar octanoyl-CoA, and measurement of concentration-dependent chemical shifts of octanoyl-CoA yielded a CMC of 30 ± 5 mM (Figure 1C).

Binding to Vesicles. The carbonyl signal from either oleoyl-CoA or octanoyl-CoA in the presence of small unilamellar PC vesicles exhibited an upfield shift from that for the micellar or monomeric forms (see Figure 1), consistent with

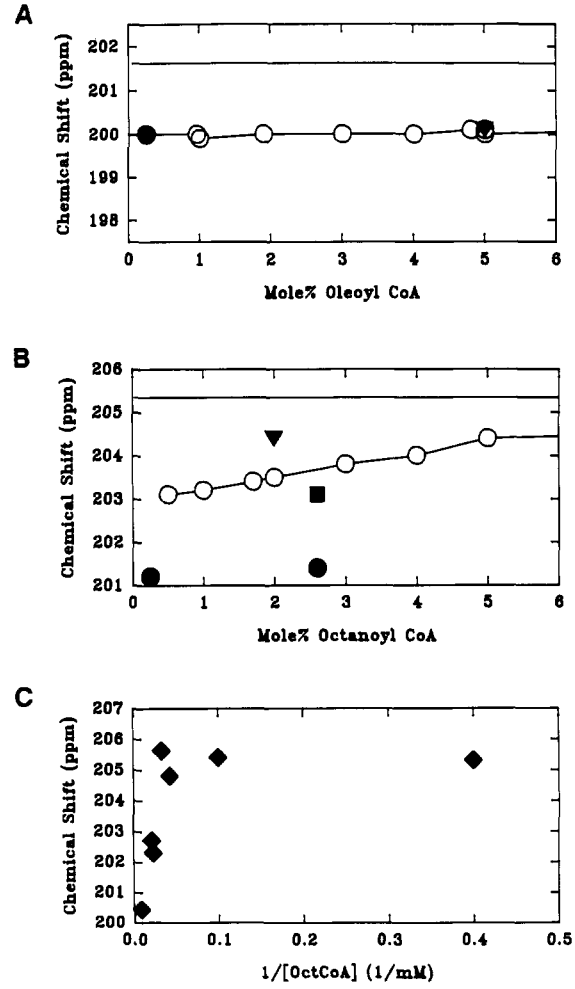

FIGURE 1: Concentration dependence of ^{13}C NMR chemical shift of thioester carbonyl for (A) oleoyl-CoA bound to small unilamellar PC vesicles, (B) octanoyl-CoA bound to PC vesicles, and (C) octanoyl-CoA in aqueous phosphate buffer. In panels A and B, symbols indicate the following PC concentrations: (●) 194.4 mg/mL, (■) 48.6 mg/mL (B only), (○) 33.3 mg/mL, and (▼) 8.3 mg/mL. Solid lines at 201.7 ppm (A) and 205.3 (B) indicate the chemical shift of micellar oleoyl-CoA and monomeric octanoyl-CoA, respectively. In panel C, the CMC of octanoyl-CoA was estimated as 30 ± 5 mM from the intersection of two lines (not shown) drawn through the data points.

incorporation of the carbonyl carbon into a more hydrophobic environment. When oleoyl-CoA was added to preformed vesicles, a single thioester peak was observed (Figures 2 and 3A) with a chemical shift (200.1 ± 0.2 ppm) that was independent of the concentration of oleoyl-CoA relative to PC up to ~15 mol % oleoyl-CoA (see Figure 1A). The carbonyl chemical shift was also independent of the absolute concentration of oleoyl-CoA in oleoyl-CoA/PC samples, since no change was observed when PC vesicles with a fixed mol % of oleoyl-CoA were diluted with buffer over a 23-fold range (Figure 1A). When vesicles were prepared by cosonication of oleoyl-CoA and PC, the carbonyl region revealed two peaks (199.8 and 200.1 ppm, Figure 3B). These chemical shifts were independent of the oleoyl-CoA/PC ratio. The peak at 200.1 ppm was much more intense than the upfield peak in all samples and represents oleoyl-CoA on the outer leaflet of the vesicle bilayer (see below). The signal from the PC carbonyls was also split into two peaks corresponding to outer and inner monolayer phospholipids (Hutton et al., 1977). Such a peak separation is seen only for small unilamellar vesicles where large differences in curvature between the outer and inner monolayer exist. On the basis of this criterion, the mixed lipid

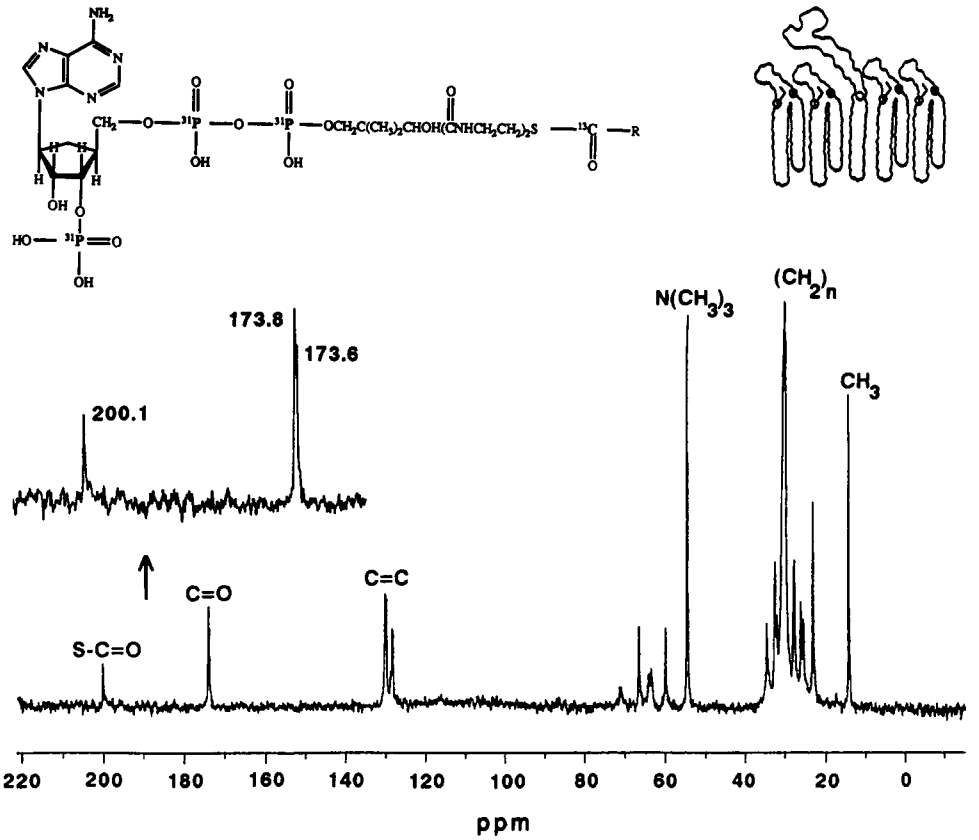

FIGURE 2: ^{13}C NMR spectrum of 1 mol % [1-^{13}C]oleoyl-CoA added to small unilamellar PC vesicles (42 mg/mL PC). The spectrum consists of 3700 accumulations with a pulse interval of 14.7 s averaged over 16 384 data points. (Inset) Thioester carbonyl (200.1 ppm) and inner (173.6 ppm) and outer (173.8 ppm) PC carbonyl signals. Selected peaks are identified: S–C=O, thioester carbonyl from oleoyl-CoA; C=O, carbonyls (outer and inner) from PC; C=C, unsaturated acyl chain carbons from PC; $N(CH_3)_3$, choline methyl carbon from PC; $(CH_2)_n$, methylene carbons from acyl chains in PC; and CH_3, terminal methyl from acyl chains in PC. Also shown (above) is the chemical structure of acyl-CoA showing the location of ^{31}P atoms and the site of ^{13}C enrichment. R represents the acyl chain. To the right of the chemical structure is a schematic representation of acyl-CoA bound to a phospholipid bilayer (only one leaflet is shown for clarity).

vesicles in this study with ≤15 mol % oleoyl-CoA contained intact bilayer vesicles, regardless of how they were prepared. Independent assessment by EM showed small vesicles (apparently unilamellar) with a narrow size distribution centered at ~300 Å. Furthermore, sonicated samples were almost clear and showed no increase in turbidity with addition of up to 15 mol % oleoyl-CoA.

In vesicles containing ≥20 mol % oleoyl-CoA, a new signal was observed at 200.7 ppm (Figure 3C). This was the predominant signal, but a smaller signal was seen at the chemical shift of oleoyl-CoA in vesicles (200.2 ppm). The carbonyl signals of PC also changed appearance at ≥20% oleoyl-CoA, showing a slightly asymmetric peak at 173.8 ppm instead of two resolved peaks at 173.8 and 173.6 ppm. Examination of such samples by EM revealed both small and large vesicles and/or multilamellar aggregates; however, the samples (all prepared by cosonication of oleoyl-CoA and PC) clarified during sonication and remained clear throughout the experiment, indicating that large aggregates were not present prior to drying and staining the sample for electron microscopy. Taken together, our data suggest that the higher oleoyl-CoA/PC ratios disrupted the lipid bilayer structure and produced mixed micelles. However, the observation of a small thioester signal (upfield shoulder) characteristic of oleoyl-CoA bound to vesicles at 200.2 ppm (Figure 3C) suggests that a fraction of the vesicles remained intact in the sample containing ≥20% oleoyl-CoA.

Oleoyl-CoA was also added to large unilamellar PC vesicles to assess the influence of vesicle size on thioester carbonyl signal(s). A broad (>50 Hz) thioester peak (200.0 ppm) was observed from large unilamellar PC vesicles containing 5 mol % oleoyl-CoA (spectrum not shown). The spectrum of the PC component was similar to that previously reported (Spooner et al., 1986); all the signals were significantly broader than those observed in small vesicle systems.

When the medium-chain octanoyl-CoA was added to small unilamellar PC vesicles, a single narrow thioester carbonyl peak was observed. In contrast to the case for oleoyl-CoA, the chemical shift of this peak was dependent on the concentration of octanoyl-CoA (see Figure 1B) and increased linearly (in the direction of the monomeric chemical shift) with increasing mol % of octanoyl-CoA. Moreover, dilution of octanoyl-CoA/PC samples with buffer resulted in a downfield chemical shift of the thioester carbonyl peak (Figure 1B), also in contrast to the oleoyl-CoA case. PC carbonyl peaks characteristic of small unilamellar phospholipid vesicles were observed for vesicles to which up to 15 mol % octanoyl-CoA was added. Higher proportions of octanoyl-CoA to PC were not studied. Examination by EM confirmed the predominance of small unilamellar vesicles.

Bilayer Distribution. As described above, two thioester carbonyl peaks were observed from vesicles made by cosonicating oleoyl-CoA and PC, and not from preformed PC vesicles to which oleoyl-CoA was added. We hypothesized that these two peaks originated from oleoyl-CoA associated with the outer and inner leaflets of the vesicles and that the peak at 200.1 ppm, the only peak observed when oleoyl-CoA was added to preformed vesicles, corresponded to oleoyl-CoA on the outer leaflet. In order to test this hypothesis, attempts were made to (i) selectively extract the oleoyl-CoA from the outer

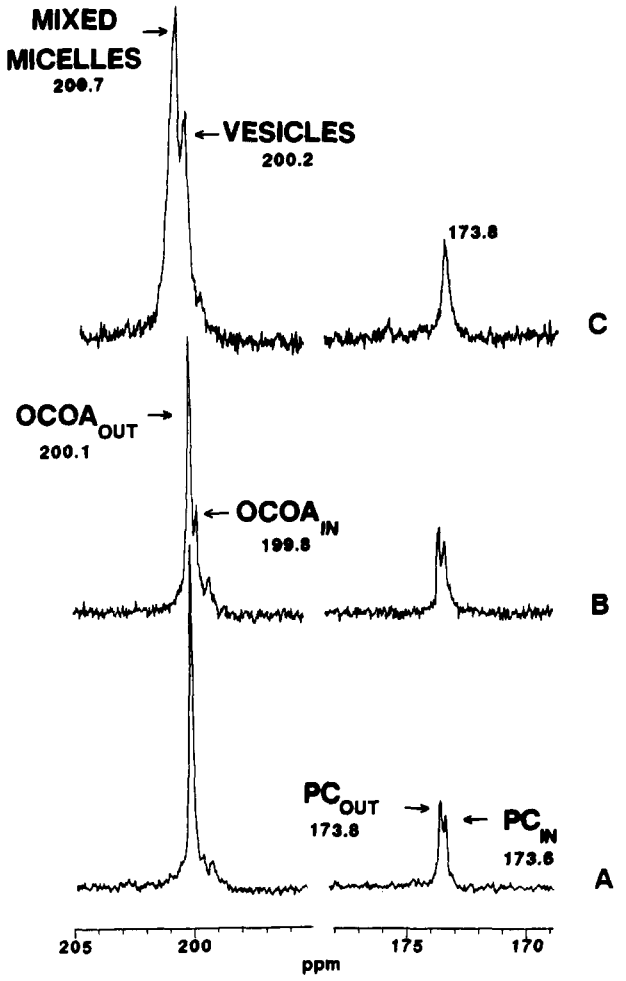

FIGURE 3: ^{13}C NMR spectrum (carbonyl region) of oleoyl-CoA (OCoA) in the presence of PC (33.3 mg/mL): (A) 7 mol % oleoyl-CoA added to preformed vesicles, (B) 7 mol % oleoyl-CoA cosonicated with PC to form small unilamellar vesicles, and (C) 20 mol % oleoyl-CoA added to preformed vesicles. Spectra were obtained as in Figure 2 except for the number of accumulations: (A and B) 3500 and (C) 5400. Spectra are scaled to give PC carbonyl signals of approximately equal intensity to allow comparison of oleoyl-CoA signal intensities.

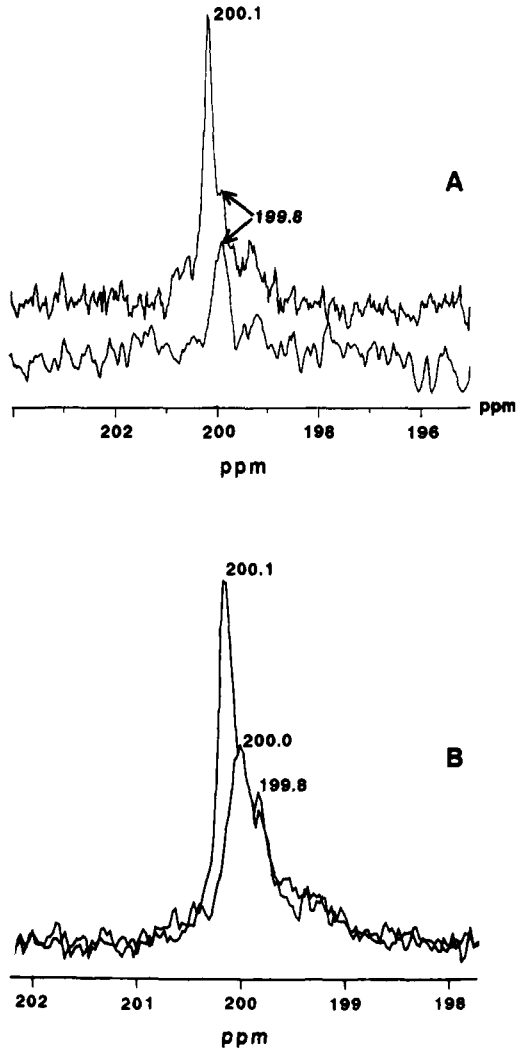

FIGURE 4: ^{13}C NMR spectra of carbonyl region of oleoyl-CoA bound to PC vesicles (7 mol % oleoyl-CoA cosonicated with 33.3 mg/mL PC in 50 mM phosphate buffer, pH 7.4). (A) Before (top) and after (bottom) addition of aqueous BSA to achieve a ratio of 3 mol of oleoyl-CoA/mol of BSA. The numbers indicate the chemical shift in ppm. The vertical scaling of the spectra in panel B is arbitrary. (B) Before (top) and after (bottom) addition of aqueous $Dy(NO_3)_3$.

leaflet with BSA and (ii) alter the chemical shift of the oleoyl-CoA on the outer leaflet with the paramagnetic lanthanide shift reagent $Dy(NO_3)_3$. In the first strategy, BSA was added to a cosonicated PC sample containing 9 mol % oleoyl-CoA. Prior to addition of BSA (top spectrum, Figure 4A), the two expected thioester carbonyl peaks (199.8 and 200.1 ppm) were observed. The downfield peak (200.1 ppm), which was approximately 3 times as intense as the upfield peak, was not detected after addition of sufficient BSA to yield a stoichiometry of 3 mol of oleoyl-CoA/per mole of BSA (bottom spectrum, Figure 4A). The chemical shift and relative intensity of the upfield peak were unchanged. Binding of oleoyl-CoA to BSA yielded [^{13}C]carbonyl signals well-separated from the signals for oleoyl-CoA bound to PC vesicles (see below). These signals are not seen in Figure 4A (bottom spectrum) because of the low signal-to-noise ratio. In the second strategy, aqueous $Dy(NO_3)_3$ (1 mol/5 mol of oleoyl-CoA) was added to a cosonicated 7 mol % oleoyl-CoA/PC sample. Prior to addition of the shift reagent (top spectrum, Figure 4B), two thioester carbonyl peaks (200.1 and 199.8 ppm) were observed with approximately a 3:1 intensity ratio (downfield/upfield peak). Following addition of $Dy(NO_3)_3$ (bottom spectrum, Figure 4B), two peaks were again observed (200.0 and 199.8 ppm). The downfield peak was broadened ~2-fold, and the intensity ratio (downfield/upfield) was reduced to ~1.5:1. The upfield peak was at the same chemical shift as the upfield peak before the $Dy(NO_3)_3$ was added. These observations are consistent with a broadening and upfield shift of the signal attributed to outer leaflet oleoyl-CoA and a lack of any effect on the inner leaflet oleoyl-CoA, from which $Dy(NO_3)_3$ was excluded.

Binding to Serum Albumin. Mixtures of oleoyl-CoA with BSA were studied by ^{13}C NMR at pH 7.4 and 35 °C. The NMR spectra exhibited three or more distinct oleoyl-CoA carbonyl signals (Figure 5), depending on the mole ratio of oleoyl-CoA to BSA. With a low ratio (1:1 oleoyl-CoA/BSA, Figure 5A), two major signals were observed (197.2 and 201.1 ppm). The peak areas of the two signals were approximately equal, although one peak (201.1 ppm) was broader and may have consisted of more than one resonance. A third peak (203.6 ppm) of much lower intensity was also observed. With a ratio of 2:1 oleoyl-CoA/BSA (Figure 5B), the intensity of the two major signals (197.1 and 201.1 ppm) increased relative to protein signals (e.g., the glutamate signal at 180.8 ppm). The relative intensity of the small peak at 203.6 ppm was apparently unchanged, but a fourth low-intensity peak (205.2 ppm) was observed. With 5:1 oleoyl-CoA/BSA (Figure 5C),

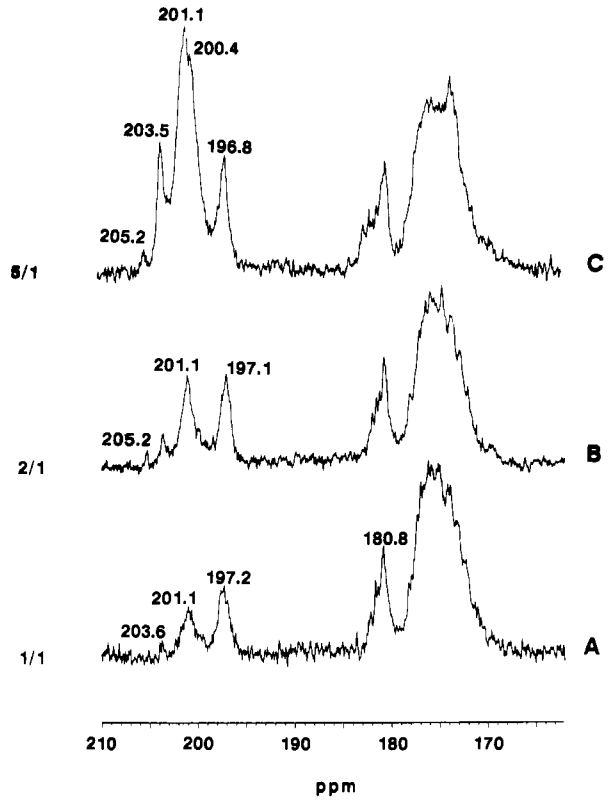

FIGURE 5: ^{13}C NMR spectrum (carbonyl region) of oleoyl-CoA bound to BSA: (A) 1:1 mole ratio oleoyl-CoA/BSA, (B) 2:1, and (C) 5:1. Spectra were obtained as in Figure 2 except the number of accumulations was 5000. The BSA concentration in aqueous phosphate buffer, pH 7.4, was 125 mg/mL in each case. The numbers indicate the chemical shift in ppm. Spectra are scaled to give protein carboxylate signals (centered at 175 ppm) of approximately equal intensity to allow comparison of oleoyl-CoA signal intensities. The peak at 180.8 ppm is from the carboxyl carbon of glutamate residues in BSA (Parks et al., 1983).

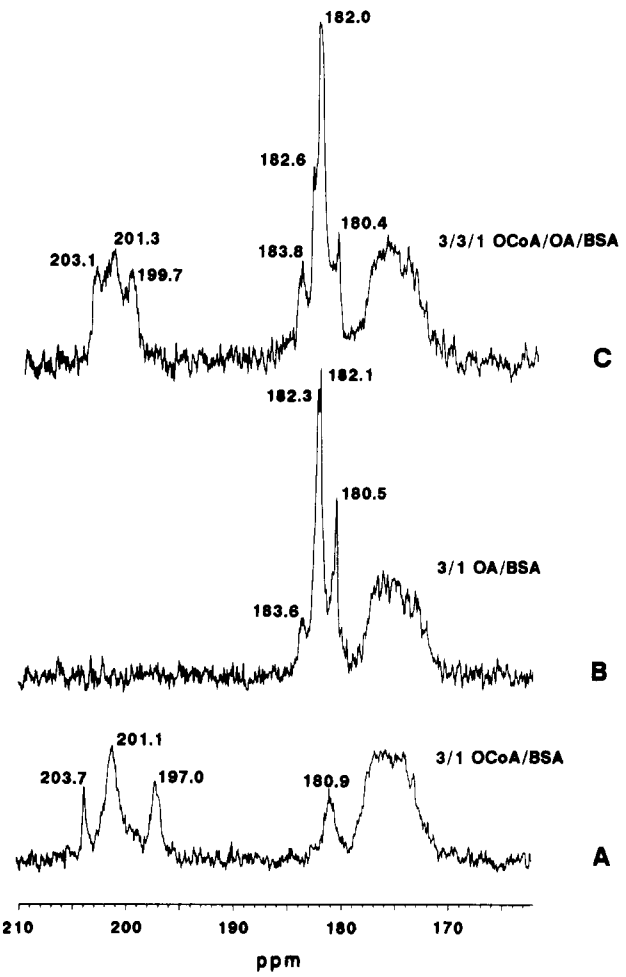

FIGURE 6: ^{13}C NMR spectrum (carbonyl region) of (A) 3 mol of oleoyl-CoA (OCoA)/mol of BSA, (B) 3 mol of oleic acid/mol of BSA, and a mole ratio of 3:3:1 OCoA/OA/BSA. For each sample, the BSA concentration was 125 mg/mL in 50 mM aqueous phosphate buffer, pH 7.4. Spectral conditions are the same as in Figure 2 except that the number of accumulations was 10000. The numbers next to peaks indicate their chemical shift (ppm).

the relative intensities of the peaks at 201.1 and 203.5 ppm increased markedly, and a fifth poorly resolved signal (200.4 ppm) was observed. This last peak may have been present (but not resolved) in spectra of samples with lower mole ratios as well. None of these signals from oleoyl-CoA corresponded to that for micellar (unbound) oleoyl-CoA (201.7 ppm). Note that the spectrum for 3:1 oleoyl-CoA/BSA (Figure 6A) shows a pattern intermediate between the 2:1 and 5:1 ratios. All five peaks seen at high mole ratios, each of which represents oleoyl-CoA in a distinct binding environment (see Discussion), were observed up to a mole ratio of 10:1.

The medium-chain thioester, octanoyl-CoA, exhibited a single peak in the presence of equimolar BSA (spectrum not shown) at 200.3 ppm, well upfield from the micellar or monomeric form. (At the concentrations used, unbound octanoyl-CoA would be monomeric.) Even with a mole ratio of 3:1 octanoyl-CoA/BSA, only a single thioester carbonyl peak (200.3 ppm) was observed. Thus, in contrast to oleoyl-CoA, multiple binding environments were not evident at 35 °C. A 2-fold dilution of this sample with buffer resulted in a slight downfield shift (0.3 ppm) of the signal. Signals for oleoyl-CoA in the presence of BSA did not shift with dilution.

Long-chain fatty acids are also known to bind to serum albumin with high affinity, and, like oleoyl-CoA, exhibit multiple carbonyl NMR signals reflecting binding to distinct sites on BSA (Parks et al., 1983; Cistola et al., 1987). Since the signals for long-chain fatty acids bound to BSA occur in a spectral region (~180–184 ppm) well-separated from oleoyl-CoA carbonyl signals, ^{13}C NMR was used to monitor binding of each lipid in the presence of the other. For example, ^{13}C-enriched oleoyl-CoA (Figure 6A) and ^{13}C-enriched oleic acid (Figure 6B), each at a 3:1 mole ratio of lipid to protein, showed characteristic multiple carbonyl signals. When these lipids were present together (3:3:1 oleoyl-CoA/oleic acid/BSA), some chemical shifts and relative signal intensities for both lipids were altered (Figure 6C). The oleic acid carbonyl spectrum showed a decrease in intensity of the peak at 180.5 ppm and an increase in intensity of the peak at 183.6 ppm. The oleoyl-CoA spectrum showed changes in chemical shift for the peaks at 203.7 and 197.0 ppm. There was no measurable decrease in the total carbonyl signal intensity (relative to the protein signal centered at 175 ppm) for either oleic acid or oleoyl-CoA. Additional ^{13}C NMR studies (data not shown) for a sample of oleoyl-CoA/BSA with a fixed mole ratio (4:1) to which increasing amounts of [^{13}C]oleic acid were added (up to 4 mol/mol of BSA) showed perturbations of both oleoyl-CoA and oleic acid signals at all compositions.

^{31}P NMR. There are three phosphorus atoms in the CoA molecule (Figure 2, top), one in a ribose phosphate which resonates downfield of H_3PO_4 and two in a pyrophosphate group which resonate upfield of H_3PO_4 as an AB quartet. Figure 7 shows ^{31}P spectra for aqueous CoA, micellar oleoyl-CoA, oleoyl-CoA bound to BSA, and oleoyl-CoA/PC mixtures at pH 7.4 ± 0.1. The pyrophosphate quartet, clearly seen for aqueous CoA (Figure 7A), was poorly resolved for

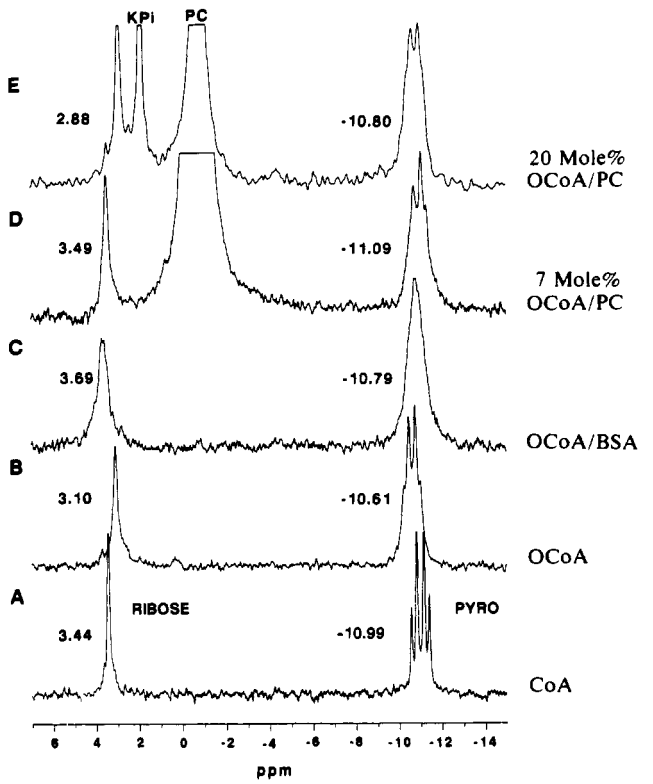

FIGURE 7: ^{31}P NMR spectrum of (A) 5 mM coenzyme A (CoA), (B) 8 mM oleoyl-CoA (OCoA), (C) 3:1 OCoA/BSA (100 mg/mL BSA), (D) 7 mol % OCoA/PC (33.3 mg/mL PC), and (E) 20 mol % OCoA/PC (33.3 mg/mL PC). Sample E was in 50 mM aqueous phosphate buffer, while samples A–D were in 50 mM KCl. All samples were at pH 7.4. Spectra consist of 1000 accumulations with a pulse interval of 2.9 s averaged over 8192 data points. Chemical shifts (numbers next to peaks) were referenced to 85% H_3PO_4 (external) at 0.00 ppm.

micellar acyl-CoA (Figure 7B) and acyl-CoA bound to PC (Figure 7D,E) and appeared as a single peak for oleoyl-CoA in the presence of BSA (Figure 7C). Thus, for the discussion which follows, a single pyrophosphate chemical shift corresponding to the center of the AB quartet is reported. In CoA, the ribose phosphate signal was at 3.44 ppm (Figure 7A), and the well-resolved quartet was centered at −10.99 ppm. In micellar oleoyl-CoA (Figure 7B), the ribose phosphate signal was observed at 3.10 ppm, and the pyrophosphate signal was centered at −10.61 ppm. In the presence of BSA (3 mol of oleoyl-CoA/mol of BSA; Figure 7C), the ribose phosphate signal (3.69 ppm) was downfield and the pyrophosphate signal (−10.79 ppm) upfield of the corresponding signals in micellar oleoyl-CoA. In contrast to the ^{13}C nucleus, the ^{31}P nuclei did not show multiple resonances for oleoyl-CoA in the presence of BSA. In oleoyl-CoA/PC mixtures containing ≤15 mol % oleoyl-CoA (e.g., Figure 7D), both the ribose phosphate signal (3.49 ppm) and the pyrophosphate signal (−11.09 ppm) occurred at different chemical shifts than the corresponding signals in micellar oleoyl-CoA. The phosphate signal from PC (−0.78 ppm) was more intense than the oleoyl-CoA phosphate signals, as expected. At ≥20 mol % oleoyl-CoA (Figure 7E), the pyrophosphate signal shifted upfield to a constant value of −10.80 ppm and the ribose phosphate signal downfield to value of 2.1–2.9 ppm, depending on the oleoyl-CoA/PC ratio.

A possible explanation for the chemical shift differences between the ribose phosphate signals of micellar oleoyl-CoA, oleoyl-CoA bound to PC vesicles, and oleoyl-CoA bound to BSA is a change in the pK_a of the ionizable ribose phosphate. To determine the apparent pK_a in each state, ^{31}P NMR spectra

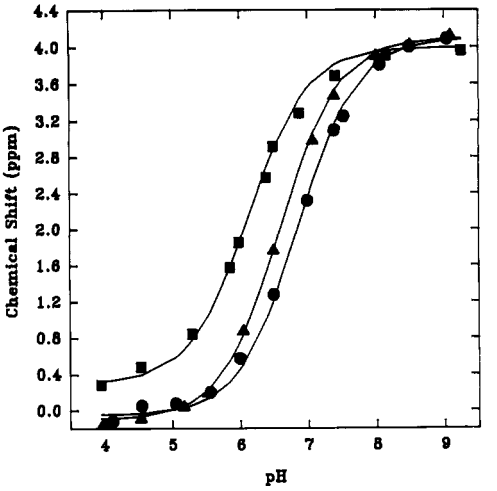

FIGURE 8: ^{31}P NMR titration curves for (■) 3:1 oleoyl-CoA/BSA (100 mg/mL BSA, (●) 4.5 mM OCoA, and (▲) 5 mol % OCoA/PC (66.9 mg/mL PC). All samples were prepared in 50 mM KCl and adjusted to pH 7.4. Curves were calculated by fitting data to the Henderson–Hasselbach equation modified for NMR titrations (see text).

were recorded at different pH values (adjusted by addition of 0.1 N KOH or HCl, as needed), and the chemical shift of the ribose phosphate was plotted as a function of pH (Figure 8). For micellar oleoyl-CoA and oleoyl-CoA bound to PC, spectra were recorded from low pH to high pH and then again at pH 7.4 to evaluate the reversibility of the pH changes. No changes in chemical shift, line width, or relative intensity compared to the original spectrum at pH 7.4 were observed. In the case of oleoyl-CoA bound to BSA, two identical samples were prepared at neutral pH, one of which was titrated to low pH and the other to high pH. The two samples were then titrated back to neutral pH, and spectra were recorded as before. While the spectra at pH 7.4 for the sample titrated to high pH were identical before and after titration, those for the sample titrated to low pH were not. The chemical shift values for the ribose phosphate were similar, but the intensity of the signal decreased with decreasing pH and remained lower than the original intensity upon titration back to pH 7.4.

The titration data (Figure 8) showed a close fit to the Henderson–Hasselbach equation (see Materials and Methods) and revealed small differences in the apparent pK_a. The value calculated for oleoyl-CoA in PC vesicles (6.59) was close to that for oleoyl-CoA in micelles (6.85), while the value for oleoyl-CoA bound to BSA was somewhat lower (6.13). Note also that the chemical shift value of the fully ionized ribose phosphate (high pH) was the same in all cases, but the chemical shift of the unionized species (low pH) differed for oleoyl-CoA bound to BSA.

Discussion

Esterification of a fatty acid to CoA results in profound changes in the nature of the fatty acid carbonyl group. The NMR chemical shift reflects a change in the electron density at the carbonyl carbon. In a thioester, the ^{13}C carbonyl chemical shift is 20–25 ppm downfield from that of an acyl ester or free fatty acid (Wehrli & Wirthlin, 1976). This large deshielding of the carbonyl carbon makes it possible to use NMR to monitor binding of both acyl-CoA and free fatty acids in mixtures modeling biological systems (see below).

Monomeric/Micellar Forms. The physical properties of fatty acids (particularly long chain) are altered when fatty acids are esterified to CoA. The complex phase behavior of fatty acids, which is dependent on several factors such as pH,

the type of counterion present, and temperature (Cistola et al., 1987), is not observed for acyl-CoA (Powell et al., 1985). Instead, acyl-CoA exists as either monomers or micelles in aqueous dispersions. ^{13}C NMR can, in principle, be used to determine the state of aggregation in aqueous dispersions since the chemical shift of the carbonyl carbon is sensitive to changes in hydration and other extrinsic factors which are altered in the monomer–micelle transition (Burns et al., 1982). In our studies, it was possible to monitor this transition for the medium-chain thioester, octanoyl-CoA. Large carbonyl chemical shift differences between the micellar and monomeric states of lipids and the downfield shift for the monomer such as those seen for octanoyl-CoA (Figure 1C) have been observed for other lipid micelles (e.g., short-chain phospholipids; Burns et al., 1982). From the concentration-dependent chemical shift (Figure 1C), we estimate the CMC of octanoyl-CoA to be 30 ± 5 mM, three orders of magnitude higher than that for oleoyl-CoA (Smith & Powell, 1986). To our knowledge, the CMC of octanoyl-CoA has not been reported; however, the results of several longer chain acyl-CoA's (12–18 carbons; Smith & Powell, 1986) showed a linear dependence of the logarithm of the CMC on chain length. Extrapolation of these data gives a value of 35 mM for the CMC of octanoyl-CoA, close to our estimate from the NMR data. Few molecular details of acyl-CoA micelle formation are known. Previous studies of palmitoyl-CoA micelles showed that the adenine groups are exposed to the aqueous environment and suggested that the hydrophobic core of the micelle begins in the region of the β-alanine moiety and includes the carbonyl (Zahler et al., 1968). Our results with micellar acyl-CoA show a partial dehydration of the carbonyl group compared to the monomer consistent with location of the carbonyl in an interfacial region.

Binding to Vesicles. Binding of oleoyl-CoA to egg PC vesicles was detected by changes in the carbonyl (^{13}C) and phosphate (^{31}P) chemical shifts relative to micellar oleoyl-CoA. In small unilamellar PC vesicles, oleoyl-CoA exhibited ^{13}C chemical shifts which differed from that of micellar oleoyl-CoA by 1.6 ppm (outer leaflet oleoyl-CoA) and 1.9 ppm (inner leaflet oleoyl-CoA). The amphipathic lipid 1-palmitoyllysophosphatidylcholine also forms micelles, and the carbonyl signal shifts upfield (~0.5 ppm) when lyso-PC goes from the micellar to PC-bound form (Bhamidipati & Hamilton, 1988). Cholic acid undergoes an upfield shift of 0.6 and 1.4 ppm between a (mixed) micelle at pH 3.0 and outer and inner leaflet locations, respectively, in small unilamellar PC vesicles (Cabral et al., 1987). These upfield [^{13}C]carbonyl shifts on going from the micellar to the PC-bound form have been interpreted as a decrease in H-bonding at the carbonyl carbon (Schmidt et al., 1978; Cabral et al., 1986). The similar change for oleoyl-CoA suggests that the acyl chain of oleoyl-CoA is packed into a more hydrophobic environment in the vesicle than in the micelle, causing a decrease in H-bonding and polarity at the carbonyl group.

In large unilamellar vesicles, binding of oleoyl-CoA was correlated with a large increase in the line width compared to that for micellar oleoyl-CoA as well as a change in chemical shift. Upon binding of oleoyl-CoA to small vesicles, only a small increase (~2-fold) in the carbonyl line width was observed. In large vesicles, most carbon atoms (even carbonyl carbons which lack directly bonded H's for efficient relaxation) exhibit broad resonances (Spooner et al., 1986). Thus, the oleoyl-CoA carbonyl peak was markedly broadened as a consequence of incorporation of oleoyl-CoA into the larger, more slowly rotating vesicles. The chemical shift of oleoyl-CoA in large unilamellar vesicles (200.0 ppm) was not significantly different from that for oleoyl-CoA on the outer leaflet of small unilamellar vesicles (200.1 ppm).

Octanoyl-CoA binding to PC vesicles, as monitored by ^{13}C NMR, was significantly different from that of oleoyl-CoA. In contrast to oleoyl-CoA, octanoyl-CoA in the presence of PC vesicles exhibited a chemical shift that was dependent on the initial octanoyl-CoA concentration in this mixture (at constant PC concentration) and on the concentration of PC at a constant octanoyl-CoA/PC ratio (Figure 1B). We considered two possible explanations for the octanoyl-CoA data: (i) all the octanoyl-CoA binds to vesicle, and the interactions change in a concentration-dependent manner, and (ii) the octanoyl-CoA partitions between water and the vesicle, and the NMR signal represents fast exchange between bound and unbound states. The latter explanation seemed more plausible because the chemical shift moved toward that for monomeric octanoyl-CoA (to higher ppm) with dilution of a vesicle sample with a fixed ratio of octanoyl-CoA/PC. Consistent with the latter explanation, Wolcowicz et al. (1982) observed both free and bound forms of pyrene-labeled butyryl-CoA in the presence of phospholipid vesicles. On the basis of measurements of the CMC of the derivatized acyl-CoA, these authors considered this probe a physical analogue of medium-chain acyl-CoA. From our data, we calculated an equilibrium binding constant by assuming the measured chemical shift reflects the ratio of bound to unbound octanoyl-CoA. The chemical shift of the monomeric octanoyl-CoA represents unbound octanoyl-CoA, and that of the most highly concentrated PC samples (194 mg/mL) was taken to represent bound octanoyl-CoA. The detection of a significant portion of octanoyl-CoA as an unbound species indicates weak binding (low affinity) of octanoyl-CoA for the bilayer. Furthermore, analysis of the narrow exchange-averaged signal (Martin et al., 1980) shows that exchange is very fast (>400 exchanges/s; lifetime <2.5 ms). Since ^{13}C NMR results showed no evidence of unbound oleoyl-CoA in the presence of PC, the affinity of oleoyl-CoA for the bilayer was much higher. Comparison of the binding of these two acyl-CoA species suggests that the acyl chain and not the CoA portion dominates the binding interactions of acyl-CoA with PC bilayers.

^{31}P NMR results are consistent with the ^{13}C NMR data, suggesting that there are no strong and specific interactions of the CoA moiety with PC. Titration of the ribose phosphate of micellar and PC-bound oleoyl-CoA showed only a small difference in the apparent pK_a (6.89 in micelles versus 6.59 in PC vesicles). This small difference in pK_a does lead to a significant difference between the chemical shifts of the two systems in the pH range of 5.5–7.5 (near the pK_a), and may account for the 0.39 ppm difference between the micellar and PC-bound ribose phosphate signal at pH 7.4 (Figure 8).

Our interpretation of NMR results for binding of acyl-CoA to PC vesicles is illustrated in Figure 2 (top). The dominant mode of binding is insertion of the acyl chain into the bilayer, the importance of which is clear from a comparison of binding of the acyl-CoA of two different chain lengths. The carbonyl carbon is partially dehydrated relative to that in the micellar structure and is probably localized in the vicinity of phospholipid carbonyls. There are still some internal mode(s) of motion available to the carbonyl group (e.g., rotation about the long the axis of the acyl chain), so that a narrow resonance is produced in small vesicles. There is no NMR evidence for strong and specific interactions of the phosphate groups.

The above results have implications for biological systems, since they show that long-chain acyl-CoA may localize in membranes near their site of synthesis or utilization while

medium-chain acyl-CoA may desorb from the membrane and equilibrate rapidly within a cell system. In ischemic conditions, where larger than normal amounts of acyl-CoA are generated, long-chain acyl-CoA would be more likely to exert deleterious effects on the lipid structure of the membrane, such as micellization. Medium-chain acyl-CoA may be less likely to reach damaging levels in membranes.

Bilayer Distribution. A single carbonyl peak (200.1 ppm) was observed when oleoyl-CoA was added to preformed vesicles, and two peaks (200.1 and 199.8 ppm) were observed when oleoyl-CoA was added to PC before sonication. The downfield peak (200.1 ppm) was assigned to oleoyl-CoA on the outer leaflet of the vesicles by several experimental criteria: only this peak and not the peak at 199.8 ppm (i) was seen when oleoyl-CoA was added to intact preformed vesicles, (ii) was broadened by a shift reagent, and (iii) disappeared after BSA was added to vesicles to bind the oleoyl-CoA.[2] Furthermore, the chemical shift separation of 0.3 ppm between carbonyl peaks of oleoyl-CoA on the two leaflets of the bilayer is similar to the chemical shift difference of other lipids in the outer and inner leaflets of bilayers, for example, phospholipids (Hutton et al., 1977), lysophospholipids (Bhamidipati & Hamilton, 1988), diacylglycerols (Hamilton et al., 1991), and bile acids (Cabral et al., 1987).[3] On the basis of the relative intensities of the outer and inner carbonyl peaks for oleoyl-CoA in vesicles prepared by cosonication, we estimate a 3:1 ratio of outer/inner leaflet oleoyl-CoA. In contrast, ^{31}P signals from oleoyl-CoA bound to PC are fairly broad and reveal no distinction between outer and inner leaflet oleoyl-CoA (Figure 7D).

Transbilayer Movement. The ability to detect narrow ^{13}C signals from oleoyl-CoA located on the two leaflets of the bilayer of small vesicles (Figures 3 and 4) also means that transbilayer movement is slow. By the criterion of chemical shift, the two peaks with a separation of 0.3 ppm (15 Hz) represent molecules whose exchange rate is much less than 15 s^{-1} (Martin et al., 1980). The kinetics of transbilayer movement can also be assessed from experiments in which oleoyl-CoA was added in low levels to preformed vesicles. In this case, even after incubation of vesicles for up to 24 h, only the signal for outer leaflet oleoyl-CoA was observed, showing that the actual rate constant is much lower than the upper limit estimated from the carbonyl chemical shift separation. Furthermore, after removal of oleoyl-CoA from the outer leaflet of vesicles by BSA, there was no indication of movement of the remaining oleoyl-CoA from the inner leaflet to the outer leaflet. Slow transbilayer movement of pyrene-labeled butyryl-CoA in vesicles was inferred from fluorescence measurements (Wolcowicz et al., 1982). In previous NMR studies, analogous to those above, negatively charged bile salt molecules present in small amounts in intact phosphatidylcholine vesicles showed no evidence of transbilayer movement (Cabral et al., 1987). The lack of measurable transbilayer movement of oleoyl-CoA is consistent with our model of the binding of oleoyl-CoA to PC bilayers in which the polar and charged groups are located in the aqueous environment. For transbilayer movement to occur, the charged groups of the CoA moiety would have to pass through the highly hydrophobic acyl chain region. Waters of hydration would either have to be shed or transported, either of which has a high activation energy (Homan & Pownall, 1988). In contrast, transbilayer movement of fatty acids (both uncharged and charged forms) in phospholipid bilayers appears to occur within hours or minutes (Gutknecht, 1988; Hamilton & Cistola, 1986), and the protonated fatty acid probably flips much faster (Hamilton & Cistola, 1986). Thus, the attachment of CoA to a long-chain fatty acid effectively anchors the acyl moiety to one side of a phospholipid bilayer. However, in complex biological membranes flip-flop could be more rapid than in PC vesicles. The heterogeneous structure may permit different binding modes for acyl-CoA or provide other mechanisms for transbilayer movement of acyl-CoA.

Membrane Disruption. Up to ~15 mol % oleoyl-CoA could be accommodated into PC vesicles without evidence of gross disruption of the bilayer structure. The ^{13}C NMR spectrum of the PC component, particularly the carbonyl region, verified the overall integrity of the small vesicles. Moreover, selective broadening of the signal for outer leaflet oleoyl-CoA in vesicles by a shift reagent (Figure 4B) also showed that the presence of this level of oleoyl-CoA did not make the vesicles leaky to, or facilitate transport of, shift reagent across the vesicle.[4] Also, our experiments showed that serum albumin was not able to penetrate the bilayer to extract oleoyl-CoA on the inner leaflet (Figure 4A). With ≥20 mol % oleoyl-CoA, stable vesicles were not obtained by our method of preparation (cosonication of lipids). The resulting structures were most likely primarily mixed micelles of PC and oleoyl-CoA, on the basis of ^{31}P and ^{13}C NMR evidence. The [^{13}C]carbonyl signal shifted downfield from the signal for intact vesicles, consistent with greater hydration of the oleoyl-CoA carbonyl group at higher oleoyl-CoA/PC ratios. The observation of a *narrow* carbonyl peak excluded the possibility of aggregation into larger structures.

With its ability to cause micellization of phospholipid bilayers at fairly low ratios, oleoyl-CoA shows a closer similarity to bile salts than to polar acyl lipids such as free fatty acids and lysophospholipids. In experiments with PC vesicles prepared as in this study, Na^+ cholate/cholic acid caused a vesicle-to-mixed-micelle transition at ~10 mol % cholate (Cabral et al., 1986). Fatty acids do not exist as micelles in aqueous solution at pH 7.4 but form acid–soap bilayers (Cistola et al., 1986); they incorporate to very high levels into phospholipids without disruption of the bilayer structure (Mabrey & Sturtevant, 1977; Pauls et al., 1983). Lyso-PC apparently can cause micellization of PC bilayers, but at least 25 mol % lyso-PC can be incorporated into PC vesicles without disruption (Kumar et al., 1989). Thus, in a comparison of the related polar intermediates in lipid metabolism, acyl-CoA, fatty

[2] Lichtenstein et al. (1982) also demonstrated removal of most but not all oleoyl-CoA in sonicated PC vesicles without apparent disruption of vesicles and inferred that only outer leaflet oleoyl-CoA was extracted. Wolcowicz et al. (1982) reached similar conclusions with pyrene-labeled butyryl-CoA. Our results provide independent corroboration of their conclusions and a more direct demonstration of the selective extraction of outer leaflet oleoyl-CoA. Our method also does not require separation of protein and vesicle complexes for determination of where acyl-CoA is bound as in Lichtenstein et al. (1982) or use of a nonnative probe as in Wolcowicz et al. (1982).

[3] The observation of two carbonyl signals for lipids in vesicles is dependent on a difference in the local magnetic environment of the carbonyl groups *and* a slow rate of transbilayer exchange. The former criterion is satisfied only when the curvature of the inner monolayer is much higher than that of the outer monolayer (i.e., in small unilamellar vesicles), which produces a measurable decrease in the hydration of lipids on the inner leaflet compared to those on the outer leaflet. The result is that the ^{13}C signal of the carbonyl group(s) on the inner leaflet is shifted upfield because of decreased H-bonding with water [Hutton et al. (1977) and references above].

[4] Although our results cannot be directly extrapolated to biomembranes, many of the effects reported for biological membranes with low levels of acyl-CoA may result from specific interactions of the acyl-CoA with other membrane constituents rather than disruption of membrane structure. Also, the phospholipid bilayer may be made leaky to molecules other than those tested here [BSA and $Dy(NO_3)_3$] as suggested by other data (Lichtenstein et al., 1982).

acids, and lysophospholipids, acyl-CoA is the most potent disrupter of bilayers. Nevertheless, our studies suggest that relatively high concentrations of acyl-CoA's can be tolerated by lipid bilayers (~15 mol %) and that only higher levels associated with certain pathological conditions are potentially disruptive.

Binding to Serum Albumin. The observation of ^{13}C and ^{31}P chemical shifts for oleoyl-CoA in the presence of BSA (Figures 5 and 8) which were different from the micellar (unbound) chemical shift and observation of line widths which were increased compared to that for micellar oleoyl-CoA demonstrate binding of oleoyl-CoA to the protein. Moreover, the observation of multiple [^{13}C]carbonyl peaks shows that oleoyl-CoA binds in structurally distinct sites on albumin and equilibrates slowly between sites. The differentiation of binding sites for oleoyl-CoA by [^{13}C]carbonyl shifts is remarkable and similar to the case for long-chain fatty acid binding to BSA (Parks et al., 1983; Cistola et al., 1987).

A recent study of binding of fluorescent-labeled acyl-CoA to BSA suggested two high and four lower affinity binding sites for this probe molecule (Richards et al., 1990). These conclusions were based on Scatchard analysis of binding data for a nonnative analogue of acyl-CoA. Our results with unmodified acyl CoA show at least four binding sites at mole ratios of ≤2:1 oleoyl-CoA/BSA, two of which have much higher affinity than the remaining two.

Our binding studies also showed that both oleic acid and oleoyl-CoA bind simultaneously to BSA. They may compete for some of the same binding sites, since binding of one detectably alters the ^{13}C signals of the other but does not produce signals for unbound lipid (Figure 6). Alternatively, binding of one lipid may alter the structure and/or affinity of a binding site for the other lipid, thus resulting in perturbations of chemical shifts. Further studies are needed to distinguish these two possibilities.

Since albumin is generally confined to the plasma compartment, under normal physiological conditions it may not contact acyl-CoA, which is located on the cytosolic side of the plasma membrane and on intracellular membranes. However, under pathological conditions such as ischemia, acyl-CoA and other polar lipids such as lysophospholipids and fatty acids are produced in higher than normal amounts (Corr et al., 1984) and may cause breakdown of the membrane structure (Haegert et al., 1987). Under these conditions acyl-CoA could be exposed to serum albumin. The fact that BSA can bind oleoyl-CoA even in the presence of oleic acid could be significant in such pathological events; i.e., albumin could remove both lipids from disrupted membranes. Finally, serum albumin is used in in vitro experiments with the goal of binding acyl-CoA to prevent adverse effects to cells (Richards et al., 1990). Unless the plasma membrane is disrupted or has mechanisms for promoting flip-flop of acyl-CoA, BSA will extract only those acyl-CoA molecules located on the monolayer of the membrane to which it is exposed.

Summary

In summary, both ^{13}C and ^{31}P NMR differentiated acyl-CoA in micellar or monomeric form, bound to PC vesicles, and bound to BSA by the criterion of chemical shift. The [^{13}C]carbonyl chemical shift provided additional details of acyl-CoA interactions with PC vesicles (localization on the two bilayer leaflets) and with BSA (differentiation of binding sites for oleoyl-CoA). The transbilayer movement (flip-flop) of acyl-CoA was too slow to be measured ($t_{1/2}$ > hours). BSA was shown to bind both oleic acid and oleoyl-CoA at levels of up to 6 mol of total lipid/mol of BSA. Octanoyl-CoA had a much lower affinity for PC bilayers than oleoyl-CoA and exchanged rapidly between bound and unbound states. The pH dependence of the ^{31}P chemical shift of the ribose phosphate group in the CoA moiety of oleoyl-CoA revealed an apparent pK_a of 6.85 in micelles. This value was little affected by binding of oleoyl-CoA to PC vesicles or to BSA.

These results suggest that in ischemia and other pathological conditions, in which high amounts of acyl-CoA are generated, long-chain acyl-CoA is more likely than medium-chain acyl-CoA to accumulate locally to potentially damaging levels in membranes. Medium-chain acyl-CoA is more likely to equilibrate rapidly throughout the cell.

Our results may have implications for the binding of macromolecules (e.g., proteins) to membranes through acylation. The 18-carbon oleoyl chain effectively anchors the larger (MW = 768) water-soluble CoA molecule to a phospholipid bilayer, while the 8-carbon octanoyl chain permits only weak and transient binding of the CoA. The length of the acyl chain (and the number of acylation sites) may control the affinity of the macromolecule for, and residence time in, a membrane.

Acknowledgments

We thank Don Gantz for the electron microscopy and Anna Tercyak for the analytical chemistry. We also thank Margaret Gibbons for preparation of the manuscript.

Registry No. Oleoyl-CoA, 1716-06-9; octanoyl-CoA, 1264-52-4; oleic acid, 112-80-1.

References

Bhamidipati, S. P., & Hamilton, J. A. (1988) *Biophys. J. 53*, 501a.

Bishop, J. E., & Hajra, A. K. (1980) *Anal. Biochem. 106*, 344–350.

Bortz, W. M., & Lynen, F. (1963a) *Biochem. Z. 337*, 505–509.

Bortz, W. M., & Lynen, F. (1963b) *Biochem. Z. 339*, 77–82.

Boylan, J. G., & Hamilton, J. A. (1990) *Biophys. J. 57*, 35a.

Burns, R. A., Roberts, M. F., Dluhy, R., & Mendelsohn, R. (1982) *J. Am. Chem. Soc. 104*, 430–438.

Burrier, R. E., & Brecher, P. (1983) *J. Biol. Chem. 258*, 12043–12050.

Cabral, D. J., Hamilton, J. A., & Small, D. M. (1986) *J. Lipid Res. 27*, 334–343.

Cabral, D. J., Small, D. M., Lilly, H. S., & Hamilton, J. A. (1987) *Biochemistry 26*, 1802–1804.

Caggiano, A. V., & Powell, G. L. (1979) *J. Biol. Chem. 254*, 2800–2806.

Canet, D., Levy, G. C., & Peat, I. R. (1975) *J. Magn. Reson. 18*, 199–204.

Cistola, D. P., Atkinson, D., Hamilton, J. A., & Small, D. M. (1986) *Biochemistry 25*, 2804–2812.

Cistola, D. P., Small, D. M., & Hamilton, J. A. (1987) *J. Biol. Chem. 262*, 10971–10979.

Corr, P. B., Gross, R. W., & Sobel, B. E. (1984) *Circ. Res. 55*, 135–154.

Gutknecht, J. (1988) *J. Membr. Biol. 106*, 83–93.

Haegert, P., Jerdonck, A., & Van Cauwelaert, F. H. (1987) *Chem. Phys. Lipids 45*, 49–63.

Hamilton, J. A. (1989) *Biochemistry 28*, 2514–2520.

Hamilton, J. A., & Small, D. M. (1981) *Proc. Natl. Acad. Sci. U.S.A. 78*, 6878–6882.

Hamilton, J. A., & Cistola, D. P. (1986) *Proc. Natl. Acad. Sci. U.S.A. 83*, 82–86.

Hamilton, J. A., Bhamidipati, S. P., Kodali, D. R., & Small, D. M. (1991) *J. Biol. Chem. 266*, 1177–1186.

Homan, R., & Pownall, H. J. (1988) *Biochim. Biophys. Acta 938*, 155-166.
Hutton, W. C., Yeagle, P. L., & Martin, R. B. (1977) *Chem. Phys. Lipids 19*, 255-265.
Janatova, J., Fuller, J. K., & Hunter, M. J. (1968) *J. Biol. Chem. 243*, 3612-3622.
Kawaguchi, A., Yoshimura, T., & Okuda, S. (1981) *J. Biochem. 89*, 337-339.
Kumar, V. V., Malewicz, B., & Baumann, W. J. (1989) *Biophys. J. 55*, 789-792.
Lichtenstein, A. H., Small, D. M., & Brecher, P. (1982) *Biochemistry 21*, 2233-2241.
Lowry, O. H., Rosebrough, N. J., Farr, A. L., & Randall, R. J. (1951) *J. Biol. Chem. 193*, 265-275.
Mabrey, S., & Sturtevant, J. M. (1977) *Biochim. Biophys. Acta 486*, 444-450.
Maggio, J. E. (1980) *Proc. Natl. Acad. Sci. U.S.A. 77*, 2582-2586.
Martin, M. L., Delpuech, J. J., & Martin, G. J. (1980) in *Practical NMR Spectroscopy*, Chapter 8, Heydem, London.
Mizuno, K., Toyosato, M., Tanimizu, I., & Hirakawa, H. (1980) *Anal. Biochem. 108*, 6.
Opella, S. J., Nelson, D. J., & Jardetzky, O. (1976) *J. Chem. Phys. 64*, 2533-2535.
Parks, J. S., Cistola, D. P., Small, D. M., & Hamilton, J. A. (1983) *J. Biol. Chem. 258*, 9262-9269.
Pauls, R. P., Mackey, A. L., & Bloom, M. (1983) *Biochemistry 22*, 6101-6109.
Powell, G. L., Tippett, P. S., Kiorpes, T. C., McMillan-Wood, J., Coll, K. E., Schulz, H., Tanaka, K., Kang, E. S., & Shrago, E. (1985) *Fed. Proc. 44*, 81-84.
Richards, E. W., Hamm, M. W., Fletcher, J. E., & Otto, D. A. (1990) *Biochim. Biophys. Acta 1044*, 361-367.
Schmidt, C. F., Barenholz, Y., Huang, C., & Thompson, T. E. (1978) *Biochemistry 16*, 3948-3954.
Shug, A. L., & Shrago, E. (1973) *J. Lab. Clin. Med. 81*, 214-218.
Smith, R. H., & Powell, G. L. (1986) *Arch. Biochem. Biophys. 244*, 357-360.
Spooner, P. J. R., Hamilton, J. A., Gantz, D. L., & Small, D. M. (1986) *Biochim. Biophys. Acta 860*, 345-353.
Sumper, M., & Trauble, H. (1973) *FEBS Lett. 30*, 29-34.
Tokayama, M., Itoh, S., Nagasaki, T., & Tanimizu, I. (1977) *Clin. Chim. Acta 79*, 93.
Wehrli, F. W., & Wirthlin, T. (1976) in *Interpretation of Carbon-13 NMR Spectra*, John Wiley & Sons, Chichester.
Whitmer, J. T., Idell-Wenger, J. A., Rovetto, M. J., & Neely, J. R. (1978) *J. Biol. Chem. 253*, 4305-4309.
Wolcowicz, P. E., Pownall, H. J., & McMillin-Wood, J. B. (1982) *Biochemistry 21*, 1990-1996.
Zahler, W. L., Barden, R. E., & Cleland, W. W. (1968) *Biochim. Biophys. Acta 164*, 1-11.

Rotational Motion of Monomeric and Dimeric Immunoglobulin E–Receptor Complexes†

Jeffrey N. Myers,‡ David Holowka, and Barbara Baird*
Department of Chemistry, Baker Laboratory, Cornell University, Ithaca, New York 14853-1301
Received May 9, 1991; Revised Manuscript Received September 5, 1991

ABSTRACT: Erythrosin 5′-thiosemicarbazide labeled immunoglobulin E (IgE) was used to monitor the rotational dynamics of monomeric and dimeric $Fc_\epsilon RI$ receptors for IgE on rat basophilic leukemia (RBL) cells using time-resolved phosphorescence anisotropy. Receptors were studied both on living RBL cells and on membrane vesicles derived from the RBL cell plasma membrane. The un-cross-linked IgE–receptor complexes on cells and vesicles exhibit rotational correlation times that are consistent with those expected for freely rotating monomers, but a small fraction of these complexes on cells may be rotationally immobile. A comparison of the initial phosphorescence anisotropy values for erythrosin-labeled IgE–receptor complexes on cells and vesicles reveals a fast component of rotational motion that is greater on the vesicles and may be due to a site of segmental flexibility in the receptor itself. Dimers of IgE–receptor complexes formed with anti-IgE monoclonal antibodies appear to be largely immobile on cells, but they are mobile on vesicles with a 2-fold larger rotational correlation time than the monomeric complexes. The results suggest that dimeric IgE–receptor complexes undergo interactions with other membrane components on intact cells that do not occur on the membrane vesicles. The possible significance of these interactions to receptor function is discussed.

Aggregation of $Fc_\epsilon RI$, the high-affinity receptor for immunoglobulin E (IgE)[1] on rat basophilic leukemia (RBL)[1] cells, results in cellular degranulation and the consequent release of histamine, as well as in the secretion of other inflammatory mediators during the allergic response [reviewed in Metzger et al. (1986), Siraganian (1988), and Beaven and Ludowyke (1989)]. The molecular mechanism by which aggregated receptors trigger a number of different signal transduction pathways that lead to these events remains largely unknown. Previous fluorescence photobleaching recovery measurements on RBL cells showed that most monomeric

† This work was supported by Grants AI18306 and AI22449 from the National Institutes of Health. J.N.M. was a predoctoral trainee of the National Institutes of Health (GM07273).
* Author to whom correspondence should be addressed.
‡ Present address: Department of Pathology, Columbia University College of Physicians and Surgeons, 630 W. 168th St., New York, NY 10032.

[1] Abbreviations: RBL, rat basophilic leukemia; IgE, immunoglobulin E; DNP, 2,4-dinitrophenyl; BSA, bovine serum albumin; IgE_m, mouse monoclonal anti-DNP IgE; IgE_r, rat myeloma IgE; IgE–R, IgE–receptor complex; Er, erythrosin 5′-thiosemicarbazide; HEPES, *N*-(2-hydroxyethyl)piperazine-*N*′-2-ethanesulfonic acid; HBS, HEPES-buffered saline.

0006-2960/92/0431-567$03.00/0